

## Microfluidic cell fragmentation for mechanical phenotyping of cancer cells

Nabiollah Kamyabi and Siva A. Vanapalli

Citation: [Biomicrofluidics](#) **10**, 021102 (2016); doi: 10.1063/1.4944057

View online: <http://dx.doi.org/10.1063/1.4944057>

View Table of Contents: <http://scitation.aip.org/content/aip/journal/bmf/10/2?ver=pdfcov>

Published by the [AIP Publishing](#)

---

### Articles you may be interested in

[Isolation of viable cancer cells in antibody-functionalized microfluidic devices](#)

[Biomicrofluidics](#) **8**, 024119 (2014); 10.1063/1.4873956

[Microfluidic devices for cell cultivation and proliferation](#)

[Biomicrofluidics](#) **7**, 051502 (2013); 10.1063/1.4826935

[Separation of tumor cells with dielectrophoresis-based microfluidic chip](#)

[Biomicrofluidics](#) **7**, 011803 (2013); 10.1063/1.4774312

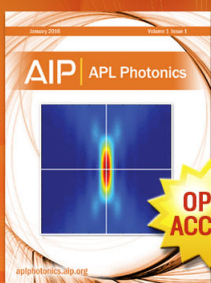
[Probing the mechanical properties of brain cancer cells using a microfluidic cell squeezer device](#)

[Biomicrofluidics](#) **7**, 011806 (2013); 10.1063/1.4774310

[Efficient capture of circulating tumor cells with a novel immunocytochemical microfluidic device](#)

[Biomicrofluidics](#) **5**, 034119 (2011); 10.1063/1.3623748

---



Launching in 2016!  
The future of applied photonics research is here

OPEN  
ACCESS

AIP | APL  
Photonics

## Microfluidic cell fragmentation for mechanical phenotyping of cancer cells

Nabiollah Kamyabi and Siva A. Vanapalli

Department of Chemical Engineering, Texas Tech University, Lubbock, Texas 79409, USA

(Received 28 January 2016; accepted 3 March 2016; published online 15 March 2016)

Circulating tumor cells (CTCs) shed from the primary tumor undergo significant fragmentation in the microvasculature, and very few escape to instigate metastases. Inspired by this *in vivo* behavior of CTCs, we report a microfluidic method to phenotype cancer cells based on their ability to arrest and fragment at a micropillar-based bifurcation. We find that in addition to cancer cell size, mechanical properties determine fragmentability. We observe that highly metastatic prostate cancer cells are more resistant to fragmentation than weakly metastatic cells, providing the first indication that metastatic CTCs can escape rupture and potentially initiate secondary tumors. Our method may thus be useful in identifying phenotypes that succumb to or escape mechanical trauma in microcirculation. © 2016 AIP Publishing LLC. [<http://dx.doi.org/10.1063/1.4944057>]

### INTRODUCTION

The hemodynamic transport of circulating tumor cells (CTCs) is an essential step in cancer metastasis.<sup>1–4</sup> It is estimated that for every gram of tumor, about a million cells are shed per day into the blood stream.<sup>5–7</sup> Despite the hematogenous dissemination of such a large number of CTCs, less than 0.01% survive to produce metastases.<sup>8–11</sup> Thus, survival of CTCs in blood circulation is a critical step for the occurrence of metastases.

The destruction of CTCs in circulation can be due to factors such as cellular anoikis and host defense mechanisms.<sup>12,13</sup> In contrast to these cytotoxic factors, several studies show that physical forces can also destroy CTCs, contributing significantly to metastatic inefficiency.<sup>14–16</sup> Further direct evidence comes from *in vivo* imaging in mouse models which show that the tumor cells arrested in the microvasculature undergo fragmentation due to fluid stresses.<sup>17–22</sup> The degree of fragmentation was found to depend on the organ site and the type of cell lines used in the animal studies.<sup>14,18,23</sup>

Inspired by the fact that CTCs are prone to mechanical destruction at microcapillary junctions, in this study we report a new microfluidic method for phenotyping cancer cells based on their fragmentation characteristics. As shown in Fig. 1, the method involves flow-induced rupture of cancer cells at a micropillar-based bifurcation, where a tumor cell is strongly stretched by fluid forces ultimately causing a portion of the cytoplasm to pinch-off. Our micropillar design builds on geometries that have been used to study droplet breakup in microfluidic devices.<sup>24–26</sup>

The method proposed here is a new addition to the growing class of techniques that harness the unique capabilities of microfluidics to phenotype tumor cells based on deformability.<sup>27–30</sup> Notable examples include squeezing of cells through microconstrictions and recording entry/passage times,<sup>31–33</sup> tracking changes to cell shape under strong extensional forces,<sup>34,35</sup> and deformability based margination.<sup>36,37</sup> However, unlike existing methods, our approach has the potential to reveal information about the ultimate fate of tumor cells, i.e., whether a tumor cell has metastatic capacity or will succumb to mechanical destruction and cell death in microcirculation. Indeed, our results show that highly metastatic cells take longer to fragment than lowly metastatic cells, suggesting that in the dynamically fluctuating microcirculatory environment, metastatic CTCs might be less prone to fragmentation.

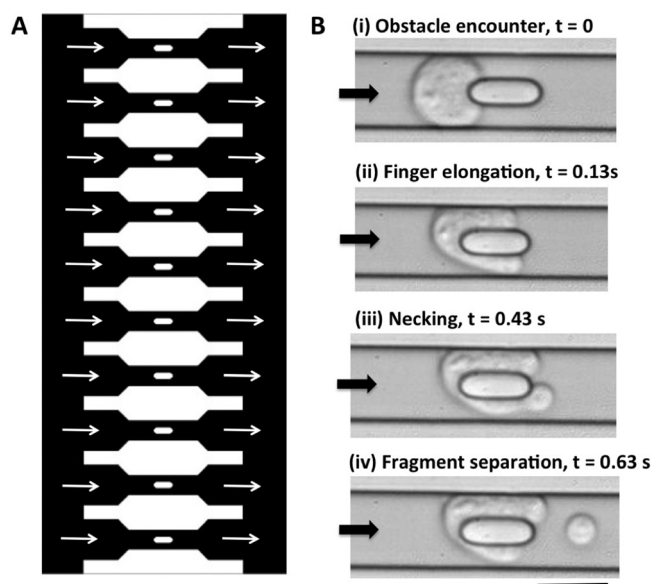


FIG. 1. Microfluidic device for flow-induced fragmentation of cancer cells. (a) The layout of the microfluidic device showing ten identical channels connected in parallel. Each channel has a micropillar that enables fragmentation of cells. (b) Time evolution of critical events underlying the fragmentation process in cancer cells. Arrows in (a) and (b) indicate the direction of fluid flow. Scale bar in (b) is  $20\ \mu\text{m}$ . (Multimedia view) [URL: <http://dx.doi.org/10.1063/1.4944057.1>]

## METHODS

Microfluidic devices were fabricated in polydimethylsiloxane using soft lithography.<sup>38</sup> The device layout consists of ten entry channels that are connected in parallel to a common inlet and outlet (Fig. 1(a)). Each of the entry channels contains a micropillar obstacle that allows flow bifurcation. The entry channel has a width of  $21.1 \pm 0.8\ \mu\text{m}$ . The obstacle has a width of  $10.9 \pm 0.7\ \mu\text{m}$  and a length of  $24.7 \pm 1.2\ \mu\text{m}$ . The gap between the micropillar and the channel wall is  $4.8 \pm 0.4\ \mu\text{m}$ . All the structures in the microfluidic device have a uniform height of  $14.5 \pm 0.6\ \mu\text{m}$ .

Two types of prostate cancer cells were used in this study—lowly metastatic LNCaP cells and highly metastatic CL2 cells. Both cells were cultured in RPMI-1640 medium (Cellgro) supplemented by 5% FBS (Fetal Bovine Serum), 1 mM L-Glutamine, 1 mM non-essential amino acids, 2 mM Sodium Pyruvate, and 1% Penicillin/Streptomycin. Cell culture chemicals were purchased from Fisher Scientific.

The microfluidic device was mounted on an inverted microscope (IX-70, Olympus Inc.). A constant pressure drop was imposed across the device using a pressure controller (MFC8-FLEX4C, Fluigent Inc.). Images were recorded with a  $20\times$  magnification objective (1 pixel =  $0.915\ \mu\text{m}$ ) using a high-speed camera (Phantom V39, Vision Research Inc.) at 500–1500 frames per second in brightfield mode. Images were analyzed manually using Image J v.1.49.

All experiments were conducted at a fixed pressure drop of 2666 Pa (= 20 mm Hg), which is within the range of intravascular pressure.<sup>39,40</sup> This pressure drop produces cell velocities of  $12 \pm 7\ \text{mm/s}$ . The fluid shear stress corresponding to this pressure drop in the micropillar gap is estimated to be  $\approx 7\ \text{Pa}$ .

## RESULTS AND DISCUSSION

In both tumor cell types, we find that the fragmentation process generally involves four steps, as shown in Fig. 1(b). When a tumor cell arrives at the obstacle (Fig. 1(b-i), Multimedia view), due to flow bifurcation it is pulled into the clearance between the pillar and the channel wall producing fingers (Fig. 1(b-ii), Multimedia view). These fingers continue to elongate over time, followed by necking of the finger (Fig. 1(b-iii), Multimedia view). The neck thins down

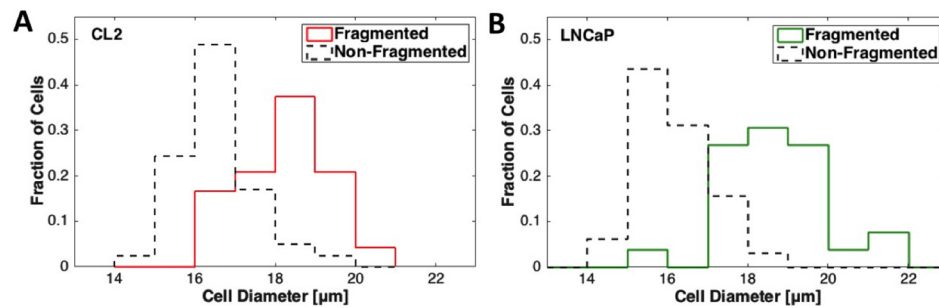


FIG. 2. Influence of cell size on fragmentability for (a) CL2 cells and (b) LNCaP cells. Even though smaller diameter cells tend to escape fragmentation, there is a considerable number of fragmented and non-fragmented (i.e., squeeze-through) cells with similar cell sizes.

ultimately causing the cytoplasmic finger to rupture and separate from the cell body (Fig. 1(b-iv), Multimedia view).

For the highly metastatic CL2 cancer cells, we find that out of 66 cells analyzed, 24 (36.4%) undergo fragmentation, while 42 (63.6%) cells squeeze through. Likewise, with the lowly metastatic LNCaP cells, out of 58 cells analyzed, 26 (45%) undergo fragmentation, while 32 (55%) cells squeeze through. These results suggest that the fragmentation is not a rare event, but a considerable number of tumor cells can rupture given suitable geometric and flow conditions.

We next investigated whether the size of the tumor cells influences their ability to fragment, since it is possible that too small a size will allow the cell to squeeze through rather than be arrested and fragmented. Consistent with this expectation, in Fig. 2, we show for both cell types, the peak of the cell diameter distribution is lower for cells that do not fragment than those that undergo fragmentation. Interestingly in both cell lines, we find a considerable overlap in the size distribution of fragmented and non-fragmented cells. In this overlap region (CL2: 16–20  $\mu\text{m}$ ; LNCaP: 15–19  $\mu\text{m}$ ), cells of similar size can either fragment or escape fragmentation by squeezing through the micropillar gap. Thus, our results show that the size alone does not influence fragmentability, but also mechanical properties of tumor cells play an important role.

Finally, we test whether the metastatic potential difference in the two cell lines can be distinguished using microfluidic fragmentation. We define two metrics—fragmentation time and excess area—to characterize the fragmentation process. Fragmentation time is the time difference between when the cell first encounters the micropillar (Fig. 1(b-i)) and when a finger separates (Fig. 1(b-iv)). We also measure the cell surface areas at these initial and final time points ( $A_o$ ,  $A_f$ ) and define the excess area,  $\Delta = (A_f - A_o)/A_o$ . Of note is that the cell surface area we measure is actually the projected area (since our imaging is two-dimensional); therefore,  $\Delta$  is an approximate measure of the degree to which the cell and its membrane are stretched. As shown in Fig. 3, we observe that the fragmentation time is higher for the more invasive cell

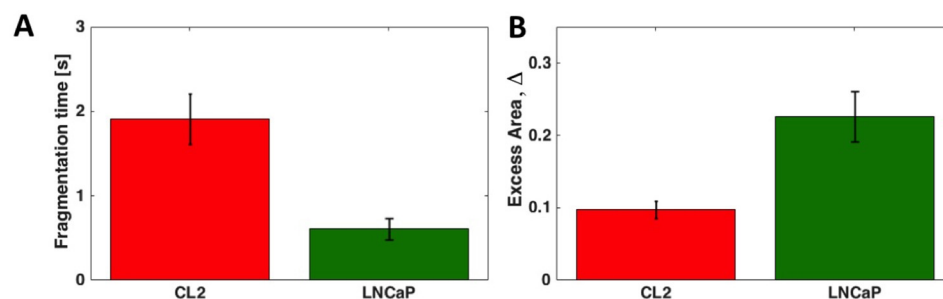


FIG. 3. Microfluidic cell fragmentation distinguishes cancer cells of different metastatic potential based on (a) fragmentation time and (b) excess area. The barplots represent mean  $\pm$  s.e.m. The Kolmogorov-Smirnov test shows the data sets are statistically significant,  $p < 0.05$ .  $n = 24$  and  $26$  for CL2 and LNCaP cells, respectively.

line CL2. The excess area, however, is less for CL2 than LNCaP cells, suggesting that the rate of membrane stretching is lower in highly metastatic cells. Thus, our fragmentation metrics are capable of differentiating prostate cancer cell lines of different metastatic potential.

In summary, we develop a new method for phenotyping cancer cells based on their fragmentation characteristics. In contrast to flow-induced squeezing of cancer cells, from a fundamental point of view, the mechanical deformation of the membrane and cytoskeleton during fragmentation is extreme, potentially lending new insights into the nonlinear mechanics of tumor cells. Additional studies are also needed to ascertain what role do mechanical properties of membrane, cytoskeleton, and nucleus play in the fragmentation process; and whether fragmented tumor cells are viable. From a methods perspective, microfluidic cell fragmentation can have a significant impact in a variety of areas, including identifying invasive phenotypes in patient samples, screening drug compounds, and generating new insights into cancer metastasis.

## ACKNOWLEDGMENTS

We acknowledge support from the Cancer Prevention and Research Institute of Texas (Grant No. RP 140298).

- <sup>1</sup>A. F. Chambers, A. C. Groom, and I. C. MacDonald, "Dissemination and growth of cancer cells in metastatic sites," *Nat. Rev. Cancer* **2**, 563–572 (2002).
- <sup>2</sup>C. L. Chaffer and R. A. Weinberg, "A perspective on cancer cell metastasis," *Science* **331**, 1559–1564 (2011).
- <sup>3</sup>I. J. Fidler, "The pathogenesis of cancer metastasis: The 'seed and soil' hypothesis revisited," *Nat. Rev. Cancer* **3**, 453–458 (2003).
- <sup>4</sup>D. Wirtz, K. Konstantopoulos, and P. C. Searson, "The physics of cancer: The role of physical interactions and mechanical forces in metastasis," *Nat. Rev. Cancer* **11**, 512–522 (2011).
- <sup>5</sup>Y. S. Chang, E. di Tomaso, D. M. McDonald, R. Jones, R. K. Jain, and L. L. Munn, "Mosaic blood vessels in tumors: Frequency of cancer cells in contact with flowing blood," *Proc. Natl. Acad. Sci. U.S.A.* **97**, 14608–14613 (2000).
- <sup>6</sup>T. P. Butler and P. M. Gullino, "Quantitation of cell shedding into efferent blood of mammary adenocarcinoma," *Cancer Res.* **35**, 512–516 (1975).
- <sup>7</sup>L. A. Liotta, J. Kleinerman, and G. M. Saidel, "Quantitative relationships of intravascular tumor cells, tumor vessels, and pulmonary metastases following tumor implantation," *Cancer Res.* **34**, 997–1004 (1974).
- <sup>8</sup>J. D. O'Flaherty, S. Gray, D. Richard, D. Fennell, J. J. O'Leary, F. H. Blackhall, and K. J. O'Byrne, "Circulating tumour cells, their role in metastasis and their clinical utility in lung cancer," *Lung Cancer* **76**, 19–25 (2012).
- <sup>9</sup>I. J. Fidler, "Metastasis: Quantitative analysis of distribution and fate of tumor emboli labeled with 125 I-5-iodo-2'-deoxyuridine," *J. Natl. Cancer Inst.* **45**, 773–782 (1970).
- <sup>10</sup>L. A. Liotta, D. Vembu, R. K. Saini, and C. Boone, "In vivo monitoring of the death rate of artificial murine pulmonary micrometastases," *Cancer Res.* **38**, 1231–1236 (1978).
- <sup>11</sup>E. Mayhew and D. Graves, "Quantitation of tumorigenic disseminating and arrested cancer cells," *Br. J. Cancer* **50**, 159–166 (1984).
- <sup>12</sup>O. Berezovskaya, A. D. Schimmer, A. B. Glinskii, C. Pinilla, R. M. Hoffman, J. C. Reed, and G. V. Glinsky, "Increased expression of apoptosis inhibitor protein XIAP contributes to anoikis resistance of circulating human prostate cancer metastasis precursor cells," *Cancer Res.* **65**, 2378–2386 (2005).
- <sup>13</sup>J. Vaage, "Humoral and cellular immune factors in the systemic control of artificially induced metastases in C3Hf mice," *Cancer Res.* **33**, 1957–1965 (1973).
- <sup>14</sup>L. Weiss, D. S. Dimitrov, and M. Angelova, "The hemodynamic destruction of intravascular cancer cells in relation to myocardial metastasis," *Proc. Natl. Acad. Sci. U.S.A.* **82**, 5737–5741 (1985).
- <sup>15</sup>L. Weiss, "Metastatic inefficiency," *Adv. Cancer Res.* **54**, 159–211 (1990).
- <sup>16</sup>K. J. Luzzi, I. C. MacDonald, E. E. Schmidt, N. Kerkvliet, V. L. Morris, A. F. Chambers, and A. C. Groom, "Multistep nature of metastatic inefficiency: Dormancy of solitary cells after successful extravasation and limited survival of early micrometastases," *Am. J. Pathol.* **153**, 865–873 (1998).
- <sup>17</sup>L. Weiss, U. Nannmark, B. R. Johansson, and U. Bagge, "Lethal deformation of cancer cells in the microcirculation: A potential rate regulator of hematogenous metastasis," *Int. J. Cancer* **50**, 103–107 (1992).
- <sup>18</sup>V. L. Morris, I. C. MacDonald, S. Koop, E. E. Schmidt, A. F. Chambers, and A. C. Groom, "Early interactions of cancer cells with the microvasculature in mouse liver and muscle during hematogenous metastasis: Videomicroscopic analysis," *Clin. Exp. Metastasis* **11**, 377–390 (1993).
- <sup>19</sup>K. Yamauchi, M. Yang, P. Jiang, N. Yamamoto, M. Xu, Y. Amoh, K. Tsuji, M. Bouvet, H. Tsuchiya, K. Tomita, A. R. Moossa, and R. M. Hoffman, "Real-time in vivo dual-color imaging of intracapillary cancer cell and nucleus deformation and migration," *Cancer Res.* **65**, 4246–4252 (2005).
- <sup>20</sup>K. Hayashi, P. Jiang, K. Yamauchi, N. Yamamoto, H. Tsuchiya, K. Tomita, A. R. Moossa, M. Bouvet, and R. M. Hoffman, "Real-time imaging of tumor-cell shedding and trafficking in lymphatic channels," *Cancer Res.* **67**, 8223–8228 (2007).
- <sup>21</sup>J. Condeelis and J. E. Segall, "Intravital imaging of cell movement in tumours," *Nat. Rev. Cancer* **3**, 921–930 (2003).
- <sup>22</sup>J. B. Wyckoff, J. G. Jones, J. S. Condeelis, and J. E. Segall, "A critical step in metastasis: In vivo analysis of intravasation at the primary tumor," *Cancer Res.* **60**, 2504–2511 (2000).
- <sup>23</sup>L. Weiss, J. Bronk, J. W. Pickren, and W. W. Lane, "Metastatic patterns and target organ arterial blood flow," *Invasion Metastasis* **1**, 126–135 (1981).



- <sup>24</sup>D. R. Link, S. L. Anna, D. A. Weitz, and H. A. Stone, "Geometrically mediated breakup of drops in microfluidic devices," *Phys. Rev. Lett.* **92**, 054503 (2004).
- <sup>25</sup>L. Salkin, L. Courbin, and P. Panizza, "Microfluidic breakups of confined droplets against a linear obstacle: The importance of the viscosity contrast," *Phys. Rev. E: Stat., Nonlinear, Soft Matter Phys.* **86**, 036317 (2012).
- <sup>26</sup>S. Protiere, M. Z. Bazant, D. A. Weitz, and H. A. Stone, "Droplet breakup in flow past an obstacle: A capillary instability due to permeability variations," *EPL-Europhys. Lett.* **92**, 54002 (2010).
- <sup>27</sup>X. Mao and T. J. Huang, "Exploiting mechanical biomarkers in microfluidics," *Lab Chip* **12**, 4006–4009 (2012).
- <sup>28</sup>Y. Zheng, J. Nguyen, Y. Wei, and Y. Sun, "Recent advances in microfluidic techniques for single-cell biophysical characterization," *Lab Chip* **13**, 2464–2483 (2013).
- <sup>29</sup>S. A. Vanapalli, M. H. Duits, and F. Mugele, "Microfluidics as a functional tool for cell mechanics," *Biomicrofluidics* **3**, 12006 (2009).
- <sup>30</sup>A. Karimi, S. Yazdi, and A. M. Ardekani, "Hydrodynamic mechanisms of cell and particle trapping in microfluidics," *Biomicrofluidics* **7**, 21501 (2013).
- <sup>31</sup>Z. S. Khan and S. A. Vanapalli, "Probing the mechanical properties of brain cancer cells using a microfluidic cell squeezer device," *Biomicrofluidics* **7**, 011806 (2013).
- <sup>32</sup>S. Byun, S. Son, D. Amodei, N. Cermak, J. Shaw, J. H. Kang, V. C. Hecht, M. M. Winslow, T. Jacks, P. Mallick, and S. R. Manalis, "Characterizing deformability and surface friction of cancer cells," *Proc. Natl. Acad. Sci. U.S.A.* **110**, 7580–7585 (2013).
- <sup>33</sup>A. Adamo, A. Sharei, L. Adamo, B. Lee, S. Mao, and K. F. Jensen, "Microfluidics-based assessment of cell deformability," *Anal. Chem.* **84**, 6438–6443 (2012).
- <sup>34</sup>D. R. Gossett, H. T. Tse, S. A. Lee, Y. Ying, A. G. Lindgren, O. O. Yang, J. Rao, A. T. Clark, and D. Di Carlo, "Hydrodynamic stretching of single cells for large population mechanical phenotyping," *Proc. Natl. Acad. Sci. U.S.A.* **109**, 7630–7635 (2012).
- <sup>35</sup>O. Otto, P. Rosendahl, A. Mietke, S. Golfier, C. Herold, D. Klaue, S. Girardo, S. Pagliara, A. Ekpenyong, A. Jacobi, M. Wobus, N. Topfner, U. F. Keyser, J. Mansfeld, E. Fischer-Friedrich, and J. Guck, "Real-time deformability cytometry: On-the-fly cell mechanical phenotyping," *Nat. Methods* **12**, 199–202 (2015).
- <sup>36</sup>Z. Liu, F. Huang, J. Du, W. Shu, H. Feng, X. Xu, and Y. Chen, "Rapid isolation of cancer cells using microfluidic deterministic lateral displacement structure," *Biomicrofluidics* **7**, 11801 (2013).
- <sup>37</sup>T. M. Geislinger and T. Franke, "Sorting of circulating tumor cells (MV3-melanoma) and red blood cells using non-inertial lift," *Biomicrofluidics* **7**, 44120 (2013).
- <sup>38</sup>Y. N. Xia and G. M. Whitesides, "Soft lithography," *Annu. Rev. Mater. Sci.* **28**, 153–184 (1998).
- <sup>39</sup>P. C. Johnson, "Effect of venous pressure on mean capillary pressure and vascular resistance in the intestine," *Circ. Res.* **16**, 294–300 (1965).
- <sup>40</sup>A. R. Pries and T. W. Secomb, in *Microcirculation*, edited by R. F. Tuma, W. N. Duran, and K. Ley (Academic Press, 2008) Chap. 1, pp. 3–36.